Open access • Journal Article • DOI:10.1007/S11085-012-9339-X

Influence of Water Vapour on the Rate of Oxidation of a Ni-25wt.%Cr Alloy at High Temperature — Source link

Patrice Berthod, Lionel Aranda, Stéphane Mathieu, Michel Vilasi

Institutions: Centre national de la recherche scientifique

Published on: 01 Jun 2013 - Oxidation of Metals (Springer-Verlag)

Topics: Wet oxidation, Oxide and Water vapor

Influence of Water Vapour on the Rate of Oxidation of a Ni–25wt.%Cr Alloy at High Temperature

Patrice Berthod, Lionel Aranda, Stéphane Mathieu, Michel Vilasi

Influence of Water Vapour on the Rate of Oxidation of a Ni-25wt.%Cr Alloy at High Temperature

Patrice Berthod, Lionel Aranda, Stéphane Mathieu, Michel Vilasi

Institut Jean Lamour (UMR CNRS 7198), Department CP2S, Faculty of Science and Technologies, Postal Box 70239, 54506 Vandoeuvre-lès-Nancy, FRANCE

Corresponding author: patrice.berthod@univ-lorraine.fr

Abstract. The effect of water vapor on the oxidation behavior of a Ni-25wt.%Cr alloy in air was studied between 1000 and 1300°C by comparing, after test in dry air and in a humidified air, mass gain results and surface / sub-surface metallographic observations. It is found that, in the conditions of the present study, the transient oxidation at the beginning of the isothermal stage and the isothermal oxidation are both slightly slower in wet air than in dry air. The oxide formed in wet air over the surface tends to be less coarse and less thick than the one formed in dry air. The chromium depletion depths in the sub-surface are similar between the two atmospheres but the concentration at the oxide / alloy interface is higher for wet air than for dry air oxidation. The oxide scale formed in wet air seems more resistant against spallation at cooling than the scale formed in dry air.

Keywords: Nickel-chromium alloy; High temperature oxidation; Water vapor; Kinetic constants; Scale characteristics

Post-print version of the article *Oxid Met (2013) 79:517–527; DOI 10.1007/s11085-012-9339-x*

INTRODUCTION

In many industrial applications water is present in the hot oxidant gases to which the metallic components can be exposed in service. This is for example the case of turbine blades used in power generation. The presence of water vapor may influence the progress of high temperature oxidation by modifying the structural characteristics of the growing external oxide scales and the kinetics of mass gain as well as of mass loss [1,2]. The chromia-forming refractory alloys or superalloys are especially concerned since, in water vapor-containing hot gases, the volatilization of their protective oxide scale is enhanced by the formation of oxy-hydroxides according to the equation ½ Cr_2O_3 (s) + H_2O(g) + ¾ O_2(g) = $CrO_2(OH)_2$(g) [1,3], with as result a decrease of the mass gain rate when the oxidation progress is followed by thermogravimetry. When the temperature is very high the volatilization of the platinum wire to which the sample is hung may also contribute to this linear mass loss by volatilization, while, one the contrary, a linear mass gain may occur in case of redeposition of a part of the previous volatilized species on the suspension in colder places of the thermobalance. It is thus important, in the mass variations recorded by the thermobalance, to separate on the one hand the parabolic contribution of the oxidation of the alloy, and on the other hand all of the linear mass losses (volatilization) or linear mass gains (recondensation), in order to better characterize the resistance of the alloy to high temperature oxidation. This uncoupling can be done for example by

evaluating the mass gain curves according to a method previously adapted to the assessment of both the parabolic and volatilization constants from the mass gain curves recorded during oxidation in dry air [4].

The aim of the present study is to test Ni25Cr-type samples cut from the same ingot obtained by equiaxed solidification, in dry air and in a humidified air with the same thermo-balance and with the same test parameters (heating and cooling rates, temperature and duration of the isothermal stage), in order to clearly reveal the differences of mass variation kinetics and the characteristics of the oxides formed (composition, external morphology, …), induced by the presence of water vapor.

EXPERIMENTAL

Several ingots of about 40 grams were elaborated from pure nickel and pure chromium (Alfa Aesar, > 99.9% of purity) by high frequency induction melting under 300mbars of pure Argon (CELES furnace, 50kW, about 4kV and 100kHz). From each of the four obtained ingots two parallelepipedic samples were cut, with as dimensions about: 10 × 10 × 3 mm^3 using a Buehler Isomet 5000 precision saw. The six faces of each parallelepiped were polished with SiC papers from 240-grid to 1200 grid, while their edges and corners were smoothed using the same 1200-grid papers.

All the thermogravimetry tests were performed with the same apparatus, a SETARAM SETSYS thermobalance, coupled with a WETSYS vapor generator device. The two samples cut in the same ingots were tested at the same temperature, one in "dry air" (no water added) and the other one in "wet air" (water added to reach 80% of relative humidity at 40°C before entering the thermobalance, i.e. about 59 mbars). The heating rate was +20°C min^{-1}, the isothermal exposures at 1000, 1100, 1200 or 1300°C was 48 hours long and the cooling rate was -5°C min^{-1}.

The thermogravimetry files were analyzed first by plotting the mass gain versus time (with the determination of the rate of the initial linear mass gain acting before the parabolic kinetic) for comparison between the two atmospheres for a same stage temperature, and second by plotting the same data but according to the $\{m \times dm/dt = Kp - K \times m\}$ scheme [4] (m: mass gain by surface unit area) in order to extract the parabolic constant Kp and the linear constant K resulting of the sum of the various linear mass gains or mass losses possibly occurring during the isothermal stage (volatilization of chromia (K_v) formed all around the sample and of the platinum of the wire (K_{Pt}), redeposition of species (K_{dep}) on the colder parts of the suspension). One can shortly remind that plotting the $\{m \times (dm/dt)\}$ quantity (unit: $g^2/cm^4/s$) versus $\{-m\}$ (unit: g/cm^2) leads, for m high enough, to a straight line the ordinate at origin of which is Kp (unit: $g^2/cm^4/s$) and the slope of which is K (unit: $g/cm^2/s$).

The oxidized samples, after cooling to room temperature, were scanned and the image obtained were subjected to image analysis (Adobe Phoshop CS) to assess the fractions of alloy surface having lost its external oxide scale by spallation, by counting the grey pixels (oxide still present) and the white pixels (metallic surface). X-Ray Diffraction was run using a Philips X'Pert Pro diffractometer (wavelength of the K_α transition of copper: λ = 1.5406 Angströms) to identify the nature of the oxides formed. Later they were coated on one side by carbon deposition to allow high magnification observation of the external morphology of the scales, using a Jeol JSM-7600F Field Emission Scanning Electron Microscope. They were thereafter coated on both sides with a thin gold layer deposited by cathodic sputtering (Fine coater JEOL JFC 1200) in order to obtain a surface electric conductivity. Subsequently, a much thicker nickel layer was deposited by electrolytic coating in a Watts bath in order to protect the oxide scale against possible deterioration during cutting. Finally the specimen was cut in two parts using the Isomet 5000 precision saw. The two halves of each oxidized sample were then embedded in a cold resin mixture (ESCIL, araldite resin CY230 + hardener HY956) and finally polished with SiC papers from 120-grit to 1200-grit, ultrasonically cleaned, and polished again, with 1µm paste to obtain a mirror-like surface state. The thickness of the oxide scales were photographed and measured using an optical microscope, while Wavelength Dispersion Spectrometry profiles were performed across the oxide scales and the alloy sub-surface in order to complete the oxide identification and to characterize the chromium-depleted zones.

RESULTS

Thermogravimetry Results

The obtained mass gain curves (examples in Figure 1) clearly show that the mass gain progress is strongly dependent on the presence of the water vapor in the oxidizing hot air, as evidenced when the two curves obtained for

a same temperature but in the two atmospheres are compared. Generally the mass gains achieved in wet air are significantly lower than the ones obtained in dry air. More precisely these differences seem to result from an enhanced volatilization as suggested by the almost horizontal end of the mass gain curves obtained in wet air. It appears thus necessary to try determining both the parabolic constant Kp and the linear kinetic constant $K=K_v+K_{Pt}+K_{dep}$, more to do not minimize Kp than to value K_v which cannot be extracted from K since K_{dep} cannot be known.

Before analyzing the "parabolic part" of the curve one can start by simply determining the linear constant K_l characterizing the end of linear oxidation at the early beginning of the isothermal stage, where the very high mass gain rate can be specified without assessment of the rates of mass loss by volatilization or mass gain by re-deposition which are not fast enough to influence the value obtained for the transient oxidation rate. The values are graphically presented in a Arrhenius plot in Figure 2, with the same scales for the values obtained in dry air (a) and in wet air (b). The points corresponding to the K_l values for the four temperatures are more (wet air) or less (dry air) on the same straight line, leading to activation energies which substantially differ (150kJ Mol^{-1} in dry air, 80kJ Mol^{-1} in wet air).

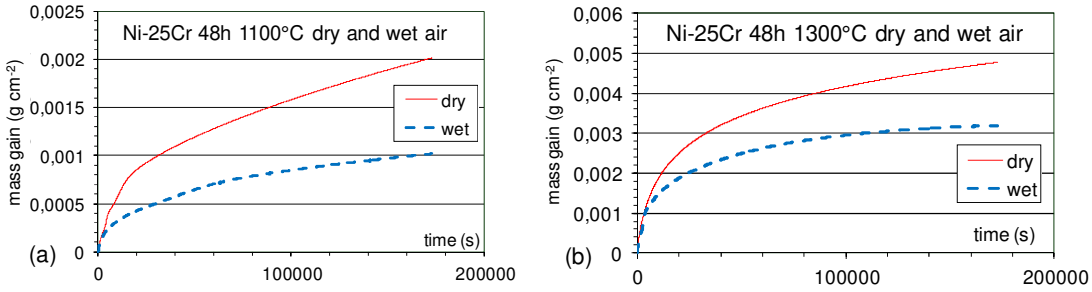

FIGURE 1. Thermogravimetry curves obtained at 1100°C (a) and at 1300°C (b) for the Ni-25Cr alloy in dry air and in wet air, showing the dependence of mass gain on the presence of water vapour

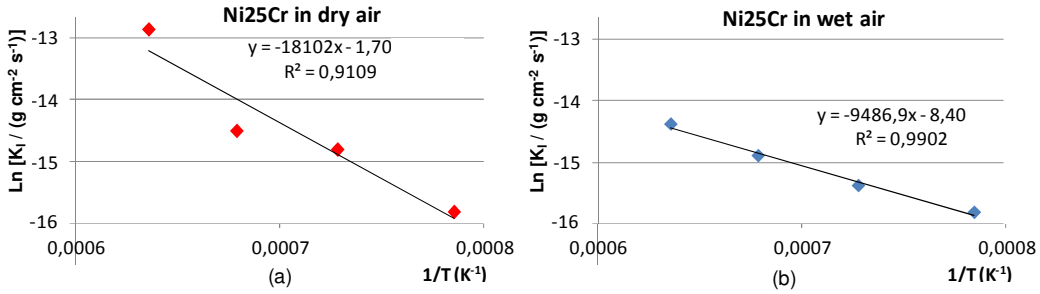

FIGURE 2. Arrhenius plot of the linear constant characterizing the transient oxidation at the beginning of the isothermal stage for the tests at 1000°C, 1100°C, 1200°C and 1300°C, in dry air (a) and in wet air (b)

The {m × dm/dt = f(m)}-plot of the mass gain files led to graphs displaying a linear part for the highest m values, the equation of which is written in each of the two graphs presented as examples in Figure 3 (1200°C/dry air (a) and 1200°C/wet air (b)). The obtained values, presented in Table 1, show that the addition of water vapor simultaneously led to a significant decrease in parabolic constant – especially at 1100 and 1200°C for which Kp is almost divided by 2 – and to an increase in linear constant K (here too especially at 1200 and 1100°C).

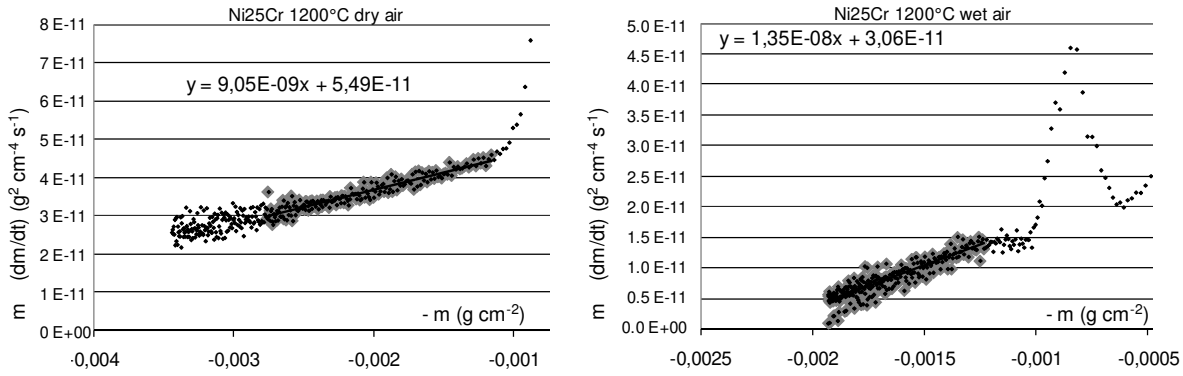

FIGURE 3. Treatment of the mass gain results according to the {m × dm/dt = Kp – K × m} method [4]

The parabolic rate constant Kp and the linear constant K both increase with the temperature of the isothermal stage. As shown by Figure 4 Kp more or less obeys a temperature dependence of an Arrhenius type in each atmosphere, but only the pre-exponential constant depends on the water vapour content since the two straight lines are parallel and thus the activation energy is almost the same for the two atmospheres (about 210kJ Mol^{-1}).

TABLE 1. Values of the parabolic constant Kp and of the constant K including all the linear mass gain variations (chromia volatilization, Pt volatilization, re-deposition), derived from the m × dm/dt = f(m) plots.

Constants	***Kp (x 10^{-12} g^2 cm^{-4} s^{-1})***		***K (=K_v+K_{Pt}+K_{dep}) (x 10^{-10} g cm^{-2} s^{-1})***	
air	dry	wet	dry	wet
1300°C	236	170	418	460
1200°C	54.9	30.6	90.5	135
1100°C	16.0	9.09	33.9	67.7
1000°C	4.82	3.51	23.5	33.5

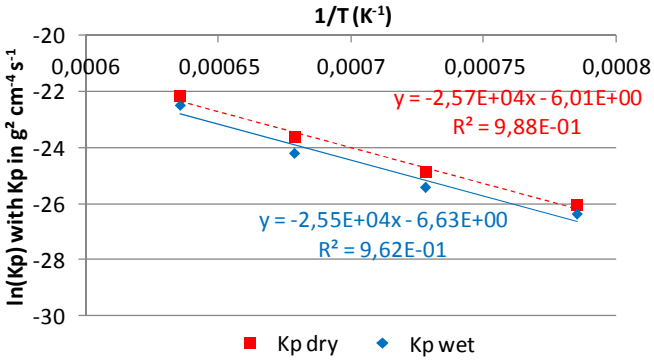

FIGURE 4. Arrhenius plot of the Kp values obtained at the four temperatures in the two atmospheres

Oxide Scale Morphology

During the cooling to room temperature the oxides scales mainly remained on the sample surfaces, although a part was locally lost on the two main faces, a phenomenon more important for a higher temperature and for dry air

than for wet air (i.e. for a thicker oxide scale), as illustrated by Figure 5 for one of the two main faces of each sample. The results of image analysis, shown in Table 2, give some data about oxide spallation.

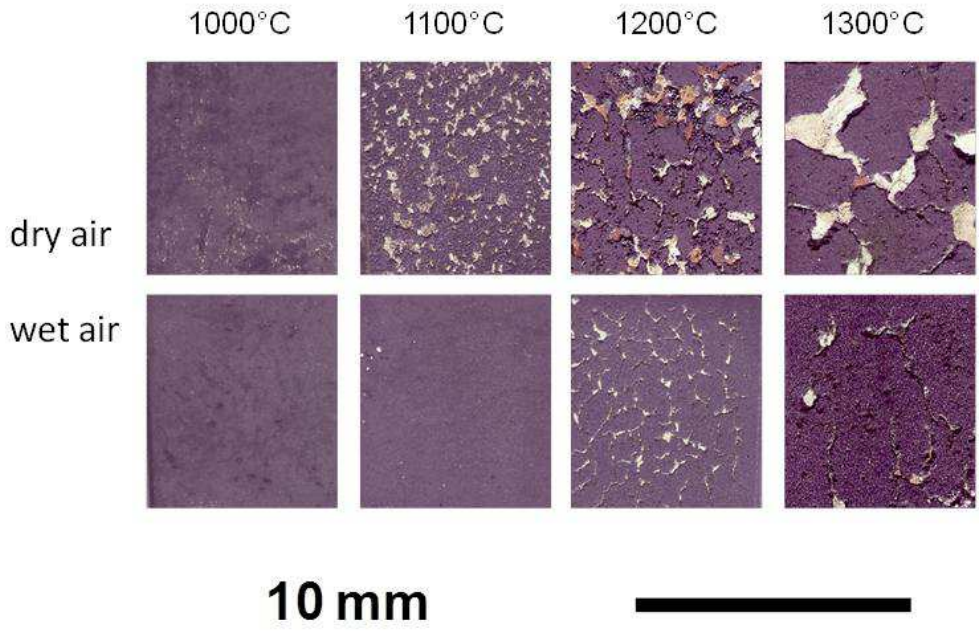

FIGURE 5. Surface states after the oxidation tests revealing the sample parts affected by oxide spallation

TABLE 2. Fractions of sample surface affected by oxide spallation during cooling, for the four temperatures of isothermal exposure and the two values of air humidity

surf.% of oxide lost by spallation	**Average ±Std deviation (σ)**	
air	dry	wet
1300°C	17.38 ±6.50	3.41 ±1.92
1200°C	13.77 ±3.22	4.25 ±0.55
1100°C	10.62 ±1.69	0.33 ±0.19
1000°C	0.77 ±0.32	0.36 ±0.16

It was also possible, after deposition of carbon to allow the use of the FEG-SEM, to examine the surfaces of the samples, essentially in the Secondary Electrons mode. As illustrated in Figure 6, the presence of water vapour induced some modifications to the external texture of the oxides formed over the samples. The samples oxidized in dry air tend to display oxide scales coarser than the ones formed in wet air. In addition, as illustrated by the XRD spectra given as examples in Figure 7, the samples oxidized in dry air generally contain several types of oxides (between 1000 and 1200°C: NiO and Cr_2NiO_4 are detected in addition to Cr_2O_3) while only chromia is present on all the samples oxidized in wet air.

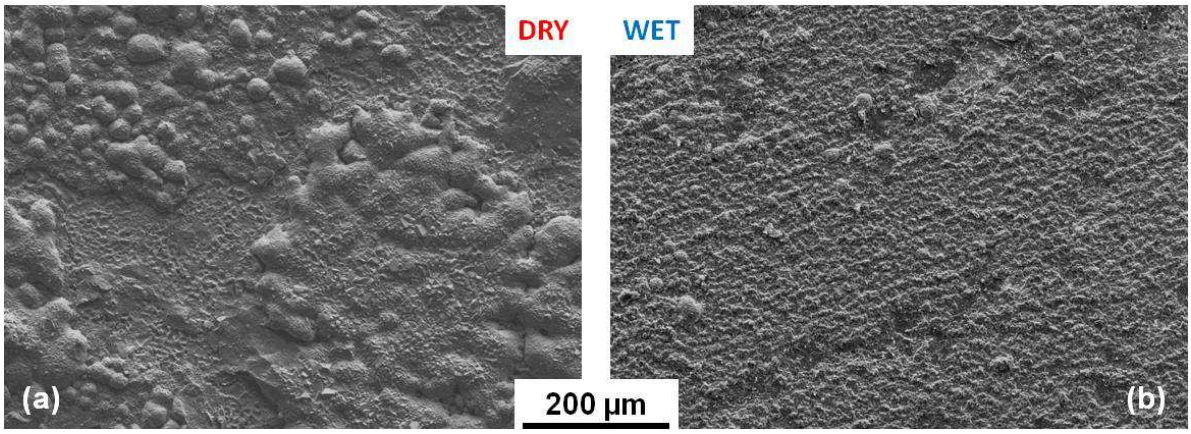

FIGURE 6. SEM micrographs of the external oxide scales after 48 hours of oxidation at 1100°C of the Ni-25Cr alloy in dry air (a) and in wet air (b)

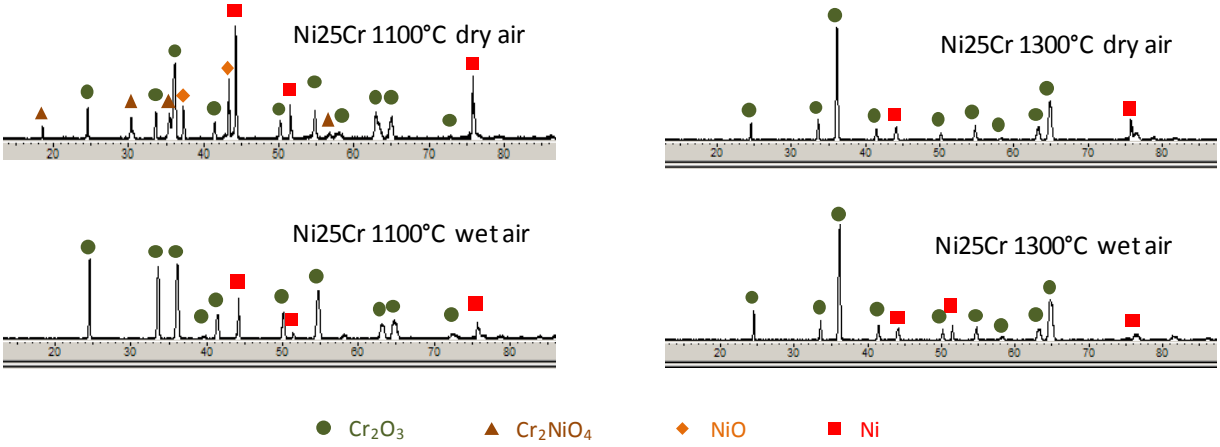

FIGURE 6. Examples of the diffraction spectra obtained on the surfaces of the external oxides

After electrolytic deposition of nickel, cutting, mounting and polishing the oxidized samples were also observed in cross-section (Figure 8). The scales appear to be thinner after oxidation in wet air than after oxidation in dry air. The oxide seems to be a little more porous in the case of wet air. The average thickness of each oxide scale was determined by measuring the thickness on micrographs taken in several locations (Table 3). The results quantitatively confirm that the scales grown in wet air are thinner than those grown in dry air.

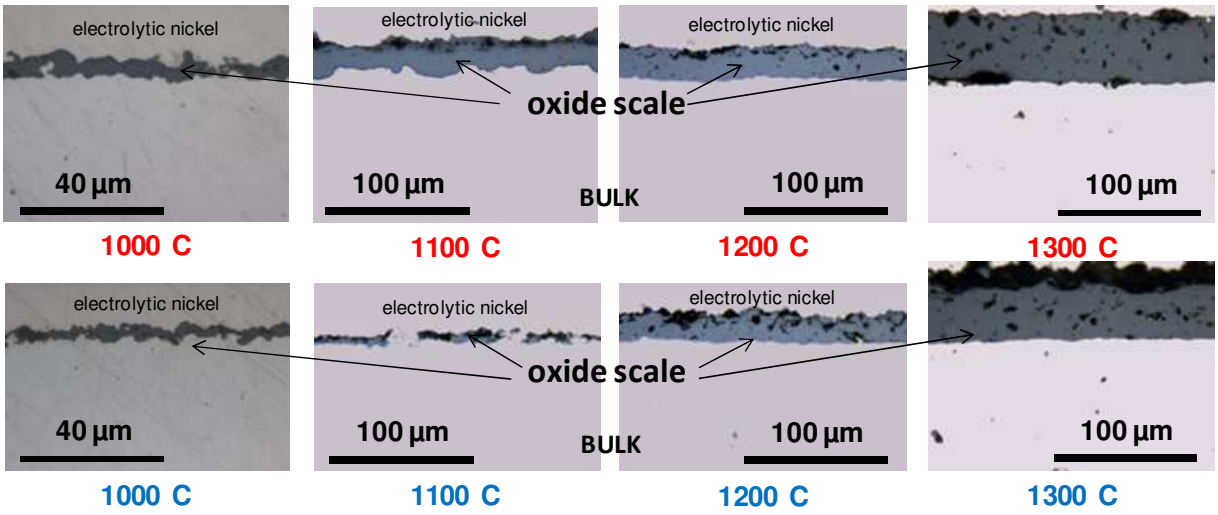

FIGURE 8. Oxide scales formed after 40 hours at the four temperatures in the two atmospheres: dry (upper micrographs) and wet (lower micrographs)

TABLE 3. Values of the thickness of external oxide (Cr_2O_3) versus oxidation temperature and air humidity

Temperature	Thickness of external oxide			
	Average ±Std deviation (σ)		Min (average - σ) – Max (average + σ)	
	dry	wet	dry	wet
1300°C	39.82 ±3.28	31.83 ±1.59	36.5 – 43.1	30.3 – 33.4
1200°C	18.83 ±1.59	16.00 ±1.48	17.3 – 20.4	14.5 – 17.5
1100°C	15.17 ±2.62	8.50 ±3.73	12.5 – 17.8	4.8 – 12.2
1000°C	5.20 ±2.21	4.73 ±3.07	3.0 - 7.4	1.7 – 7.8

The WDS profiles of chromium concentrations first confirmed the additional presence of nickel oxides and of nickel-chromium oxides in the scales developed on the samples exposed to dry air contrary to the ones oxidized in wet air. They also allowed characterizing the new chromium distribution in the sub-surface affected by oxidation. First, as illustrated in Figure 9, the minimum Cr content in the alloy at the oxide/alloy interface tends to be higher after oxidation in wet air than after oxidation in dry air (Table 4). For wet air the average Cr-gradient, assessed as the slope of the regression straight line of the Cr-content profile in the Cr-depleted zone, is also generally lower than for dry air (Table 4). The same observation can be made concerning the depth depleted in chromium (Table 5). This finally results in a chromium mass having left the alloy which is of course higher for higher temperature but also lower after oxidation in wet air than after oxidation in dry air (Table 5), this being in full agreement with the order of the real Kp values (i.e. corrected from chromia volatilization) between dry air and wet air (Table 1).

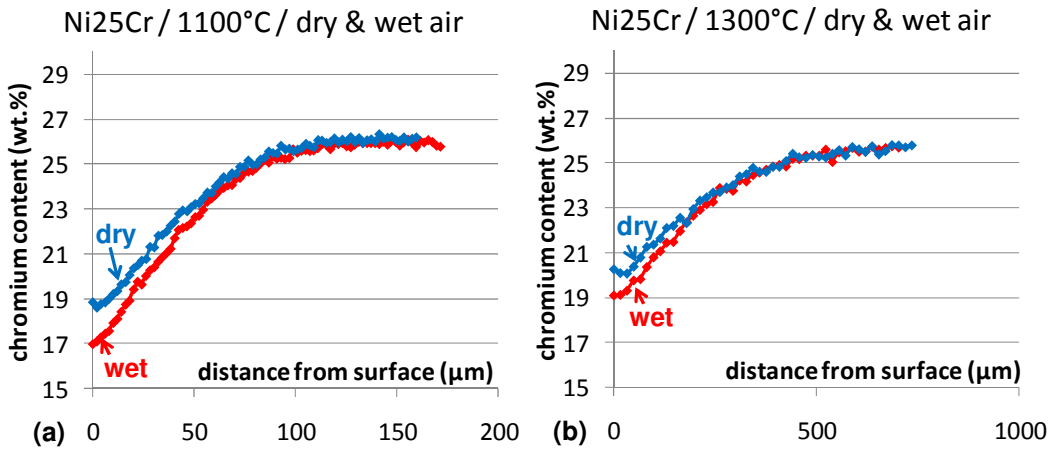

FIGURE 9. WDS chromium profiles across the sub-surfaces of the Ni-25Cr samples after 48 hours of oxidation at 1100°C (a) and at 1300°C (b)

TABLE 4. Chromium content in extreme surface and average chromium gradient (slope of the regression straight line of the linear part of the profile) across the Cr-depleted zone versus oxidation temperature and air humidity

Temperature	Surface Cr content (wt.%)		Cr gradient (10^{-3} wt.% µm^{-1})	
	dry	wet	dry	wet
1300°C	19.1*	19.7-20.3	19.3*	16.2 – 16.3
1200°C	20.8 - 21.1	20.2 - 20.3	32.4 – 33.8	34.2 – 34.3
1100°C	17.0 - 18.5	18.8 - 21.1	120 - 136	60 - 106
1000°C	16.5 - 19.1	19.1 - 21.8	264 - 378	111 - 253

*: only one WDS profile was realized

TABLE 5. Depth depleted in chromium and mass of chromium lost by the alloy versus the oxidation temperature and the air humidity

Temperature	Chromium depletion			
	Cr-depleted depth (µm)		Cr mass lost (mg cm^{-2})	
	dry	wet	dry	wet
1300°C	490*	408 - 506	10.9*	9.58 – 9.60
1200°C	211 - 220	194 - 198	4.43 – 4.67	3.98 – 4.33
1100°C	101 - 105	93 - 99	2.90 – 3.10	2.09 – 2.69
1000°C	32 - 48	32 - 42	0.88 - 1.21	0.91 – 0.99

*: only one WDS profile was realized

DISCUSSION

Many studies have been done concerning the effect of water vapour on the high temperature oxidation behaviour of metallic alloys. As generally mentioned the presence of water vapor in the oxidizing air significantly modifies the mechanisms of oxidation as well as the oxidation rates. In this work achieved on a material strictly controlled, a Ni-25Cr alloy especially elaborated and displaying a solidified microstructure totally free of any plastic deformation (differently from cold rolled samples for example) and with exactly the same chemical composition and cutting orientation of the two samples exposed at the same temperature but one in dry air and the other one in wet air, the comparison between the two atmospheres was absolutely direct, the possible emerging differences having to be necessary attributed to the water vapour content. It appeared first that the mass gain curves obtained at a same temperature but for the two atmospheres were very different from one another. This was first observed concerning the values of the linear constants K_l (at the early beginning of isothermal stage) for which one noticed for all tests a systematically lower rate in wet air than in dry air, with in addition a very marked difference of activation energy. Unfortunately the available elements did not allow interpreting such difference and an extension of this study may include in situ XRD measurements during the heating end and in the beginning of the isothermal stage.

Another kinetic difference concerns the parabolic constant Kp which was significantly lower in wet air than in dry air. This order, which is inverse to some of the other studies previously carried out related to the effect of water vapor – notably [5] which concerned also a Ni-25Cr alloy but forged/hot rolled instead cast – is confirmed by the comparison of the thicknesses of the external oxides, as well as by the chromium masses having left the alloy deduced from the WDS profiles. However it is true that the $\{m \times dm/dt = K_p - K_v \times m\}$ method [4] was developed by considering that the linear kinetic constant only concerns the Cr_2O_3 volatilized from the oxide scale present on the sample, while the constant K determined here does not include only K_v but also other terms (notably K_{dep}). By reminding in addition that other oxides (of Ni and of Ni + Cr) also formed on this Ni-25Cr in dry air, this leads to the fact that the chromia volatilization K_v constant was not accurately determined and then that the {chromia volatilization}–corrected K_p constant is not here determined with a very high accuracy. Nevertheless the trend concerning K_p is obviously good and one can also think that K_v varies with the air humidity in the same way as the global K value.

It was here interesting to see that the presence of water vapor allowed the samples to be covered by only chromia while other oxides existed in addition on the samples oxidized in dry air, this in addition to the difference of apparent fineness of the most external part of the oxide. The latter point, as well as the better adherence of the oxide formed in wet air, are phenomena which were previously reported by [5] as well as in many other studies (e.g. [6]).

CONCLUSION

The presence of water vapor in hot air, which is generally known to have a great importance on the high temperature oxidation behavior of the alloys, generally in the bad way, obviously had rather a positive influence in the present case, i.e. for the studied cast Ni-25Cr alloy and for the studied water vapour concentration. Indeed the oxidation rate was slowed (but the chromia-volatilization rate probably accelerated), as shown by the thermogravimetry data, oxides thicknesses and quantifications of alloy's chromium consumption. Furthermore the oxides were of pure chromia, showed a finer morphology, and a significantly better adherence on the substrate, an important point for alloys which are exposed to thermal cycling. After these observations one can imagine that it can be interesting to artificially enrich hot air with a precise quantity of water to improve both the isothermal oxidation resistance of such alloy and its resistance against cycling oxidation. However these observations need to be enriched by additional investigations, including for example in situ XRD measurements during certain periods of oxidation for better characterizing the mechanisms of oxidation and their differences between dry and wet atmosphere. In addition technical improvements of the thermogravimetric device are required for avoiding the re-deposition of volatile species and for allowing a more direct assessment of the chromia volatilization constant.

ACKNOWLEDGMENTS

The authors wish to gratefully thank the Common Service of Electronic Microprobe and Microanalyses, especially Sandrine Mathieu (FEG-SEM examinations) and Olivier Rouer (WDS Microprobe measurements), as well as Pascal Villeger (XRD runs).

REFERENCES

1. D.Young, *High Temperature Oxidation and Corrosion of Metals*, Amsterdam: Elsevier Corrosion Series, 2008.
2. S. R. J. Saunders, M. Monteiro and F. Rizzo, *Progress in Materials Science*. **53**, 775 (2008).
3. H. Buscail, R. Rolland, C. Issartel, F. Rabaste, F. Riffard, L. Aranda and M. Vilasi, *Journal of Materials Science*. **46**, 5903 (2011).
4. P. Berthod, *Oxidation of Metals.* **64**, 235 (2005).
5. J. Zurek, D. J. Young, E. Essuman, M. Hänsel, H. J. Penkalla, L. Niewolak, W. J. Quadakkers, *Materials Science and Engineering A*. **477**, 259 (2008).
6. M. Michalik, M. Hansel, J. Zurek, L. Singhheiser, W. J. Quadakkers, *Mat. High Temp.* **22**, 213 (2005).